The initial state of ultra-relativistic heavy ion collision

V.K. Magas*, L.P. Csernai,*,† and D.D. Strottman $^{\ddagger,\diamond}$

*Section for Theoretical and Computational Physics, Department of Physics
University of Bergen, Allegaten 55, 5007 Bergen, Norway
† KFKI Research Institute for Particle and Nuclear Physics
P.O.Box 49, 1525 Budapest, Hungary
‡ Theoretical Division, Los Alamos National Laboratory,
Los Alamos, NM, 87454, USA
$^\diamond$ Institut für Theoretische Physik, Universität Frankfurt
Robert-Mayer-Str. 8-10, D-60054 Frankfurt am Main, Germany

A model for energy, pressure and flow velocity distributions at the beginning of ultra-relativistic heavy ion collisions is presented, which can be used as an initial condition for hydrodynamic calculations. Our model takes into account baryon recoil for both target and projectile, arising from the acceleration of partons in an effective field, $F^{\mu\nu}$, produced in the collision. The typical field strength (string tension) for RHIC energies is about $5-12\,GeV/fm$, what allows us to talk about "string ropes". The results show that a QGP forms a tilted disk, such that the direction of the largest pressure gradient stays in the reaction plane, but deviates from both the beam and the usual transverse flow directions. Such initial conditions may lead to the creation of "antiflow" or "third flow component" [17].
PACS numbers: 25.75.-q, 24.85.+p, 25.75.Ld, 24.10.Jv.

1 Introduction

Fluid dynamical models are widely used to describe ultra-relativistic heavy ion collisions. Their advantage is that one can vary flexibly the Equation of State (EoS) of the matter and test its consequences on the reaction dynamics and outcome. In energetic collisions of large heavy ions, especially if a Quark-Gluon Plasma (QGP) is formed in the collision, one-fluid dynamics is a valid and good description for the intermediate stages of the reaction. Here, interactions are strong and frequent, so that other models, (e.g. transport models, string models, etc., assuming binary collisions, with free propagation of constituents between collisions) have limited validity. On the other hand, the initial and final, Freeze-Out (FO), stages of the reaction are outside the domain of applicability of the fluid dynamical model.

In conclusion, the realistic, and detailed description of an energetic heavy ion reaction requires a Multi Module Model, where the different stages of the reaction are each described with suitable theoretical approach. It is important that these Modules are coupled to each other correctly: on the interface, which is a 3 dimensional hyper-surface in space-time with normal $d\sigma^\mu$, all conservation laws should be satisfied (e.g. $[T^{\mu\nu} d\sigma_\nu] = 0$), and entropy should not decrease, $[S^\mu d\sigma_\mu] \geq 0$. These matching conditions were worked out and studied for the matching at FO in detail in refs. [1, 2, 3].

After hadronization and FO, matter is already dilute and can be described well with kinetic models.

The initial stages are more problematic. Frequently, two or three fluid models are used to remedy the difficulties and to model the process of QGP formation and thermalization [4, 5, 6]. Here the problem is transferred to the determination of drag-, friction- and transfer- terms among the fluid components, and a new problem is introduced with the (unjustified) use of an EoS in each component in a nonequilibrated situations, where an EoS does not exist. Strictly speaking this approach can only be justified for mixtures of noninteracting ideal gas components. Similarly, the use of transport theoretical approaches assuming dilute gases with binary interactions is questionable, as, due to the extreme Lorentz contraction in the C.M. frame, enormous particle and energy densities with the immediate formation of perturbative vacuum should be handled. Even in most parton cascade models these initial stages of the dynamics are just assumed in form of some initial condition, with little justification behind.

Our goal in the present work is to construct a model, based on the recent experiences gained in string Monte Carlo models and in parton cascades. One important conclusion of heavy ion research in the last decade is that standard 'hadronic' string models fail to describe heavy ion experiments.

All string models had to introduce new, energetic objects: string ropes [7, 10], quark clusters [8], fused strings [9], in order to describe the abundant formation of massive particles like strange antibaryons. Based on this, we describe the initial moments of the reaction in the framework of classical (or coherent) Yang-Mills theory, following ref. [11] assuming a larger field strength (string tension) than in ordinary hadron-hadron collisions. For example calculations in the Quark Gluon String Model (QGSM) indicate that the energy density of strings reaches $8 - 9\ GeV/fm$ already in SPS reactions. In addition we now satisfy all conservation laws exactly, while in the literature up to now and also in ref. [11] infinite projectile energy was assumed, and so, overall energy and momentum conservation was irrelevant. Thus, in this approach for the first time the initial transparency/stopping and energy deposited into strings and "string ropes" will be determined consistently with each other. We do not solve simultaneously the kinetic problem leading to parton equilibration, but assume that the arising friction is such that the heavy ion system will be an overdamped oscillator, i.e. yo-yoing of the two heavy ions will not occur, as all recent string and parton cascade results indicate.

2 Formulation of model

Our basic idea is to generalize the model developed in [11], for collisions of two heavy ions and improve it by strictly satisfying conservation laws [12, 13]. First of all, we would create a grid in the $[x, y]$ plane (z – is the beam axes, $[z, x]$ – is the reaction plane). We will describe the nucleus-nucleus collision in terms of steak-by-streak collisions, corresponding to the same transverse coordinates, $\{x_i, y_j\}$. We assume that baryon recoil for both target and projectile arise from the acceleration of partons in an effective field $F^{\mu\nu}$, produced in the interaction. Of course, the physical picture behind this model should be based on chromoelectric flux tube or string models, but for our purpose we consider $F^{\mu\nu}$ as an effective abelian field. The single phenomenological parameter we use to describe this field must be fixed from comparison with experimental data.

We describe the streak-streak collision using conservation laws:

$$\partial_\mu \sum_i T_i^{\mu\nu} = \sum_i F_i^{\nu\mu} n_{i\mu} \ , \tag{1}$$

$$\partial_\mu \sum_i n_i^\mu = 0 \ , \quad i = 1, 2 \ , \tag{2}$$

where n_i^μ is the baryon current of ith nucleus. We are working in the Center of Rapidity Frame (CRF), which is the same for all streaks. The concept of using target and projectile reference frames has no advantage any more. We will use the parameterization:

$$n_i^\mu = \rho_i u_i^\mu \ , \quad u_i^\mu = (\cosh y_i, \ \sinh y_i) \ . \tag{3}$$

$T^{\mu\nu}$ is the energy-momentum flux tensor. It consists of five parts, corresponding to both nuclei and free field energy (also divided into two parts) and one term defining the QGP perturbative vacuum.

$$T^{\mu\nu} = \sum_i T_i^{\mu\nu} + T_{pert}^{\mu\nu} = \sum_i \left[e_i \left(\left(1 + c_0^2\right) u_i^\mu u_i^\nu - c_0^2 g^{\mu\nu} \right) + T_{F,i}^{\mu\nu} \right] + B g^{\mu\nu} \ , \quad i = 1, 2 \ . \tag{4}$$

Here B is the bag constant, the equation of state is $P_i = c_0^2 e_i$, where e_i and P_i are energy density and pressure of QGP.

In complete analogy to electro-magnetic field

$$F_i^{\mu\nu} = \partial^\nu A_i^\mu - \partial^\mu A_i^\nu = \begin{pmatrix} 0 & -\sigma_i \\ \sigma_i & 0 \end{pmatrix} \ , \tag{5}$$

$$\sigma_i = \partial^3 A_i^0 - \partial^0 A_i^3 \ , \tag{6}$$

$$T_{F,i\mu\nu} = -g_{\mu\nu}\mathcal{L}_{F,i} + \sum_\beta \frac{\mathcal{L}_{F,i}}{\partial\left(\partial^\mu A_i^\beta\right)}\partial_\nu A_i^\beta \quad , \tag{7}$$

$$\mathcal{L}_{F,i} = -\frac{1}{4}F_{i\mu\nu}F_i^{\mu\nu} \ . \tag{8}$$

In our case the string tensions, σ_i, will have the same absolute value σ and opposite sign (in complete analogy to the usual string with two ends moving in opposite directions), and σ_i will be constant in the space-time region after string creation and before string decay.

To get the analytic solutions of the above equations, we use lightcone variables

$$(z,t) \to (x^+, x^-), \quad x^\pm = t \pm z \ . \tag{9}$$

Following [11], we insist that $e_1, y_1, \rho_1, A_1^\mu$ are functions of x^- only and $e_2, y_2, \rho_2, A_2^\mu$ depend on x^+ only.

In terms of lightcone variables:

$$n_i^\pm = n_{i,\mp} = \rho_i(u_i^0 \pm u_i^3) = \rho_i e^{\pm y_i} \ , \tag{10}$$

$$\begin{pmatrix} T_i^{++} & T_i^{+-} \\ T_i^{-+} & T_i^{--} \end{pmatrix} = \begin{pmatrix} h_{i+}e^{2y_i} & h_{i-} \\ h_{i-} & h_{i+}e^{-2y_i} \end{pmatrix} + T_{F,i} \ , \tag{11}$$

where

$$h_{i+} = (1+c_0^2)e_i \ , \quad h_{i-} = (1-c_0^2)e_i \ . \tag{12}$$

$$\begin{pmatrix} F_i^{++} & F_i^{+-} \\ F_i^{-+} & F_i^{--} \end{pmatrix} = \begin{pmatrix} 0 & 2\sigma_i \\ 2\sigma_i & 0 \end{pmatrix} \ . \tag{13}$$

$$T_{pert} = \begin{pmatrix} 0 & 2B \\ 2B & 0 \end{pmatrix} \ . \tag{14}$$

At the time of the first touch of two streaks, $t = 0$, there is no string tension. We assume that strings are created, i.e. the sting tension achieves the value σ at time $t = t_0$, corresponding to complete penetration of streaks through each other (see Fig. 1).

3 Conservation laws and string creation

In lightcone variables eq. (2) may be rewritten as

$$\partial_- n_1^- + \partial_+ n_2^+ = 0 \ . \tag{15}$$

So, we have a sum of two terms, depending on different independent variables, and the solution can be found in the following way:

$$\begin{array}{ll} \partial_- n_1^- = a, & \partial_+ n_2^+ = -a \ , \\ n_1^- = ax^- + (n_1)_0, & n_2^+ = -ax^+ + (n_2)_0 \ . \end{array} \tag{16}$$

Since both n_1^- and n_2^+ are positive (and also more or less symmetric) we can conclude that for our case $a = 0$.

Finally

$$n_1^- = \rho_1 e^{-y_1} = \rho_0 e^{y_0} \ , \quad n_2^+ = \rho_2 e^{y_2} = \rho_0 e^{y_0} \ , \tag{17}$$

$$\rho_1 = \rho_0 e^{y_0 + y_1} \ , \quad \rho_2 = \rho_0 e^{y_0 - y_2} \ . \tag{18}$$

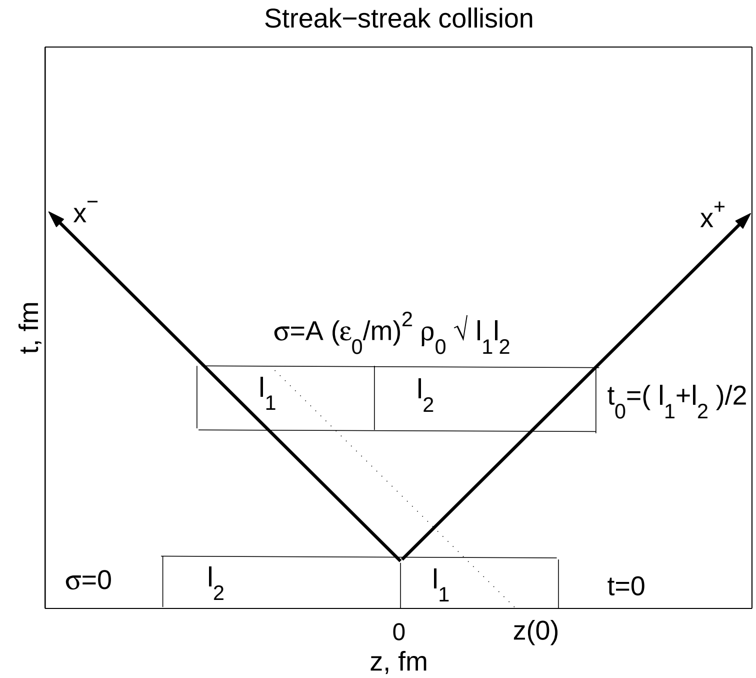

Figure 1: Streak-streak collision. $t = 0$ at the time of first touch of streaks. $t = t_0$ corresponds to complete penetration of streaks through each other. At this time strings are completely created, i.e. string tension reaches an absolute value $\sigma = A\left(\frac{\varepsilon_0}{m}\right)^2 \rho_0\sqrt{l_1 l_2}$ (22).

Let us come back to the energy-momentum tensor $T^{\mu\nu}$. Based on eqs. (6, 7, 8) and taking into account the Lorentz gauge, $\partial^0 A_i^0 - \partial^3 A_i^3 = 0$, we can find

$$\begin{pmatrix} T_{F,i}^{++} & T_{F,i}^{+-} \\ T_{F,i}^{-+} & T_{F,i}^{--} \end{pmatrix} = \begin{pmatrix} \sigma_i^2 - 2\sigma_i\left(\partial^0 A_i^0\right) + 2\sigma_i\left(\partial^3 A_i^0\right) & 0 \\ 0 & \sigma_i^2 + 2\sigma_i\left(\partial^0 A_i^0\right) + 2\sigma_i\left(\partial^3 A_i^0\right) \end{pmatrix} . \tag{19}$$

As mentioned before, after string creation, i.e. $t > t_0$, and before string decay we choose the string tensions in the form:

$$\sigma_2 = -\sigma_1 = \sigma > 0 \, . \tag{20}$$

To satisfy the above choice and the Lorentz gauge condition we take the vector potentials in the following form:

$$\begin{array}{ll} A_1^+ = 0, & A_1^- = -2\sigma x^- \, , \\ A_2^+ = -2\sigma x^+, & A_2^- = 0 \, . \end{array} \tag{21}$$

In our calculations we used the parameterization:

$$\sigma = A\left(\frac{\varepsilon_0}{m}\right)^2 \rho_0\sqrt{l_1 l_2} \, , \tag{22}$$

where l_1 and l_2 are the initial streak lengths (see Fig. 1). We are working in the system, where $\hbar = c = 1$, so σ has a dimension of $length^{-2} = energy/length$. The typical values of dimensionless parameter A are around $0.045 - 0.055$. The above parameterization is arbitrary in the sense that the requirements of the right dimension and grid size independence do not completely fix it. The above parameterization has been checked to work in the energy range $\varepsilon_0 = 10 - 3000\ GeV$ per nucleon. Notice, that there is only one free parameter in parameterization (22). The typical values of σ are $5 - 12\ GeV/fm$ for $\varepsilon_0 = 100\ GeV$ per nucleon. These values are consistent with the energy density in non-hadronized strings, or "latent energy density" which is on the average 8 GeV/fm^3.[14, 15, 16]

The problem with eq. (1) is that we do not know what the really conserved quantities are. Using the definition of $F^{\mu\nu}$, eq. (6), we can rewrite eq. (1) as

$$\partial_\mu T^{\mu\nu} = \sum_i F_i^{\mu\nu} n_{i,\mu} = \sum_i \left(\partial^\mu \left(A_i^\nu n_{i,\mu}\right) - A^\nu \partial^\mu n_{i,\mu} - \partial^\nu \left(A_i^\mu n_{i,\mu}\right) + A^\mu \partial^\nu n_{i,\mu}\right) \ . \tag{23}$$

The solutions for n_1^- and n_2^+, eq. (17), show that the second and fourth terms vanish. So, we can define new energy-momentum tensor $\tilde{T}^{\mu\nu}$, such that

$$\partial_\mu \tilde{T}^{\mu\nu} = 0 \ , \tag{24}$$

$$\tilde{T}^{\mu\nu} = \sum_i \tilde{T}_i^{\mu\nu} + T^{\mu\nu}_{pert} = \sum_i \left(T_i^{\mu\nu} - A_i^\nu n_i^\mu + g^{\mu\nu} A_i^\alpha n_{i\alpha}\right) + B g^{\mu\nu} \tag{25}$$

Using the exact definition of A_i^μ – eqs. (21) – we obtain

$$\tilde{T}^{\mu\nu} = \begin{pmatrix} h_{1+}e^{2y_1} + 5\sigma^2 & h_{1-} + 4\sigma x^- n_1^+ \\ h_{1-} + 2\sigma x^- n_1^+ & h_{1+}e^{-2y_1} + \sigma^2 - 2\sigma x^- n_1^- \end{pmatrix} + \begin{pmatrix} h_{2+}e^{2y_2} + \sigma^2 + 2\sigma x^+ n_2^+ & h_{2-} - 2\sigma x^+ n_2^- \\ h_{2-} - 4\sigma x^+ n_2^- & h_{2+}e^{-2y_2} + 5\sigma^2 \end{pmatrix}$$
$$+ \begin{pmatrix} 0 & 2B \\ 2B & 0 \end{pmatrix} . \tag{26}$$

Now the new conserved quantities are

$$Q_0 = \int \tilde{T}^{00} dV = \triangle x \triangle y \sum_i \int_{l_i} \tilde{T}_i^{00} dz \ , \tag{27}$$

$$Q_3 = \int \tilde{T}^{03} dV = \triangle x \triangle y \sum_i \int_{l_i} \tilde{T}_i^{03} dz \ , \tag{28}$$

where the volume integral runs over the lengths of the both streaks and $\triangle x \triangle y$ is the cross section of the streaks.

Based on conservation of Q_0, Q_3 we can calculate rapidity, energy and baryon densities at the moment $t = t_0$, when the string with tension σ is created. These new quantities are used as initial conditions for our differential eqs. (1, 2). As shown in the appendix A –

$$\left(\frac{\varepsilon_1(t_0)}{m}\right) = \left(\frac{\varepsilon_0}{m}\right) \frac{1}{1+c_0^2} - \frac{\sigma^2}{\rho_0\varepsilon_0(1+c_0^2)} \frac{l_1+5l_2}{4l_1} - \frac{\sigma e^{y_0}}{8\varepsilon_0(1+c_0^2)}(l_1+2l_2) - \frac{B}{\rho_0\varepsilon_0(1+c_0^2)} \frac{l_1+l_2}{2l_1} \ , \tag{29}$$

$$\left(\frac{\varepsilon_2(t_0)}{m}\right) = \left(\frac{\varepsilon_0}{m}\right) \frac{1}{1+c_0^2} - \frac{\sigma^2}{\rho_0\varepsilon_0(1+c_0^2)} \frac{l_2+5l_1}{4l_2} - \frac{\sigma e^{y_0}}{8\varepsilon_0(1+c_0^2)}(l_2+2l_1) - \frac{B}{\rho_0\varepsilon_0(1+c_0^2)} \frac{l_1+l_2}{2l_2} \ . \tag{30}$$

Here the ε_i is energy per nucleon in CRF. Now the proper baryon density and γ_i can be found, $\rho_i(t_0) = \rho_0 \frac{\varepsilon_0}{\varepsilon_i(t_0)}$, $\gamma_i = \frac{1}{\sqrt{1-v_i^2}} = \frac{\varepsilon_i(t_0)}{m}$.

For $x^\pm > x_0$ we should solve eqs. (24), with boundary conditions

$$\begin{aligned} &n_1^\pm(x^- = x_0) = \rho_0 e^{\mp y_0} && n_2^\pm(x^+ = x_0) = \rho_0 e^{\pm y_0} \\ &h_{1+}(x^- = x_0) = e_1(t_0)(1+c_0^2) && h_{2+}(x^+ = x_0) = e_2(t_0)(1+c_0^2) \\ &y_1(x^- = x_0) = y_1(t_0) && y_2(x^+ = x_0) = y_2(t_0) \\ &\sigma_1(x^- = x_0) = -\sigma && \sigma_2(x^+ = x_0) = \sigma \ , \end{aligned} \tag{31}$$

where $x_0 = 2t_0 - |z(0)|$ defines the string creation surface $t = t_0$, for nucleon or cell element in the position $z = z(0)$ at the time $t = 0$, and $e_i(t_0) = m\rho_i(t_0)$ – energy density in the rest frame.

Let us present the complete analytical solution in the following form (for detailed calculations see App. B)

$$e^{(-)^{i+1}2y_i} = -\frac{d_i}{b_i} + \left(\frac{d_i}{b_i} + e^{(-)^{i+1}2y_i(t_0)}\right)\left(1 - \frac{x^i - x_0}{\tau_i}\right)^{-\frac{b_i}{\alpha a_j}} , \tag{32}$$

$$h_{i+} = e^{(-)^{i+1}2y_i} e_i(t_0)(1 + c_0^2) e^{-(-)^{i+1}2y_i(t_0)} \left(1 - \frac{x^i - x_0}{\tau_i}\right) , \tag{33}$$

$$\rho_i = \rho_0 e^{y_0} e^{(-)^{i+1}y_i} , \tag{34}$$

where $x^1 = x^-,\ x^2 = x^+$, $i, j = 1, 2\ ,\ i \neq j,$ and the notations are from App. B (68,70,74-76).

Then the trajectories of nucleons (or cell elements) for both nuclei are given by:

$$\begin{gathered} x_1^+(x^-) = z(0) + \int_{t_0}^{x^-} dx\ e^{2y_1(x)} = \\ x_0 - \tfrac{d_1}{b_1}(x^- - x_0) + \left(\tfrac{d_1}{b_1} + e^{2y_1(t_0)}\right)\tau_1 \tfrac{\alpha a_2}{2\sigma\rho_0 e^{y_0}}\left[\left(1 - \tfrac{x^- - x_0}{\tau_1}\right)^{-\frac{2\sigma\rho_0 e^{y_0}}{\alpha a_2}} - 1\right] , \end{gathered} \tag{35}$$

$$\begin{gathered} x_2^-(x^+) = -z(0) + \int_{t_0}^{x^+} dx\ e^{-2y_2(x)} = \\ -z(0) - \tfrac{d_2}{b_2}(x^+ - x_0) + \left(\tfrac{d_2}{b_2} + e^{-2y_2(t_0)}\right)\tau_2 \tfrac{\alpha a_1}{2\sigma\rho_0 e^{y_0}}\left[\left(1 - \tfrac{x^+ - x_0}{\tau_2}\right)^{-\frac{2\sigma\rho_0 e^{y_0}}{\alpha a_1}} - 1\right] , \end{gathered} \tag{36}$$

for nucleon or cell element in the position $z = z(0)$ at the time $t = 0$.

4 Recreation of matter

As we may see from the trajectories, eqs. (35, 36), nucleons (or cell domains) will keep going in the initial direction up to the time $t = t_{i,turn}$, then they will turn and go backwards until the two streaks again penetrate through each other and new oscillation will start. Such a motion is analogous to the "Yo-Yo" motion in the string models. Of course, it is difficult to believe that such a process would really happen in heavy ion collisions, because of string decays, string-string interactions, interaction between streaks and other reasons, which are quite difficult to take into account. To be realistic we should stop the motion described by eqs. (35, 36) at some moment before the projectile and target cross again.

We assume that the final result of collisions of two streaks, after stopping the string's expansion and after its decay, is one streak of the length $\triangle l_f$ with homogeneous energy density distribution, e_f, and baryon charge distribution, ρ_f, moving like one object with rapidity y_f. We assume that this is due to string-string interactions and string decays. As was mentioned above the typical values of the string tension, σ, are of the order of 10 GeV/fm, and these may be treated as several parallel strings. The string-string interaction will produce a kind of "string rope" between our two streaks, which is responsible for final energy density and baryon charge homogeneous distributions. Notice that decay of our "string rope" does not allow charges to remain at the ends of the final streak, as it would be if we assume full transparency.

The homogeneous distributions are the simplest assumptions, which may be modified based on experimental data. Its advantage is a simple expression for $e_f,\ \rho_f,\ y_f$.

The final energy density, baryon density and rapidity, $e_f,\ \rho_f$ and y_f, may be determined from conservation laws.

$$\cosh^2 y_f = \frac{(M^2(1+c_0^2) + 2c_0^2) + \sqrt{(M^2(1+c_0^2) + 2c_0^2)^2 + 4c_0^4(M^2 - 1)}}{2(1+c_0^2)(M^2 - 1)} , \tag{37}$$

where we neglected $B \triangle l_f$ next to $Q_0/\triangle x \triangle y$ and introduced the notation $M = (l_2 + l_1)/(l_2 - l_1)$,

$$e_f = \frac{\frac{Q_0}{\triangle x \triangle y} - B \triangle l_f}{((1 + c_0^2)\cosh^2 y_f - c_0^2) \triangle l_f} \ , \tag{38}$$

$$\rho_f = \frac{\rho_0 (l_1 + l_2)}{\triangle l_f} \ . \tag{39}$$

It is interesting to analyze equation (37), which gives y_f, as a function of l_1 and l_2. If l_1 or $l_2 \ \rightarrow \ 0$ then $M \rightarrow 1$ and $|y_f| \rightarrow \infty$ (in this case $\triangle l_f \rightarrow \infty$ also, so we can not neglect $B \triangle l_f$, and y_f of course can not be larger then y_0) – no stopping, because there is no reason to stop. If $l_1 \rightarrow l_2 \quad M \rightarrow \infty$ and $y_f \rightarrow 0$ – complete stopping.

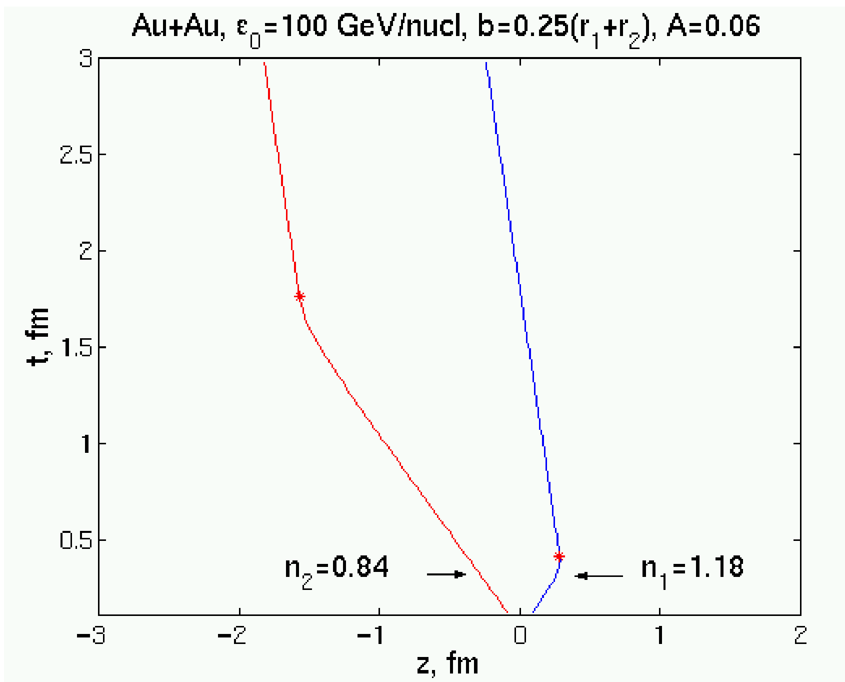

Figure 2: The typical trajectory of the ends of two initial streaks, corresponding to numbers of nucleons, n_1 and n_2. Stars denote the points, where $y_i = y_f$. From t_0 till those streak ends keep going according to eqs. (35, 36). Later the final streak starts to move like one object with rapidity, y_f, eq. (37) in CRF.

The typical trajectory of the streak ends is presented in Fig. 2. From t_0 they move according to eqs. (35, 36) until they reach the rapidity $y_i = y_f$. Later the final streak starts to move like one object with rapidity y_f.

The time and position of final streak formation can be found from the condition:

$$y_i = y_f \ , \tag{40}$$

which gives for the ith nucleus $(x_1 = x^-, \ x_2 = x^+)$

$$x_{i,\ final} = t_0 + \tau_i \left[1 - \left(\frac{\frac{d_i}{b_i} + e^{(-)^{i+1} 2 y_i(t_0)}}{\frac{d_i}{b_i} + e^{(-)^{i+1} 2 y_f}} \right)^{\frac{\alpha a_j}{b_i}} \right] \ . \tag{41}$$

5 Initial conditions for hydrodynamic calculations

In this section we present the results of our calculations. We are interested in the shape of QGP formed, when string expansions stop and their matter is locally equilibrated. This will be the initial state for further hydrodynamic calculations. The time, τ, at which we assume to reach local equilibrium and to start hydrodynamic description, is a second (after A) free parameter of our model. Of course, τ should be larger than the time of final streak formation, at least in the central most hot and dense region. For the peripheral streaks the string tension is low, and the transparency is large, but peripheral matter does not play a leading role in further hydrodynamic expansion. So, to have a homogeneous output for each streak-streak collision, we will also build the final streaks ($y_f,\ \rho_f,\ e_f$) for peripheral streak-streak collisions, with lengths, $\triangle l_f$, corresponding the lengths of the interacting region at the moment $t = \tau$, even if the final rapidity, y_f, was not achieved yet for this particular collision.

We may see in Figs. 3, that finally a QGP forms a tilted disk for $b \neq 0$. Thus, the direction of fastest expansion, the same as largest pressure gradient, will be in the reaction plane, but will deviate from both the beam axis and the usual transverse flow direction. So, the new flow component, called "antiflow" or "third flow component" [17], will appear in addition to the usual transverse flow component in the reaction plane. With increasing beam energy the usual transverse flow is getting weaker, while this new flow component is strengthened. The mutual effect of the usual directed transverse flow and this new "antiflow" or "third flow component" contribute to an enhanced emission in the reaction plane. This was actually observed and studied earlier. One should also mention that both the standard transverse flow and new "antiflow" contribute to "elliptic flow".

6 Conclusions

Based on earlier Coherent Yang-Mills field theoretical models and introducing effective parameters, based on Monte-Carlo string cascade and parton cascade model results, a simplified model is introduced to describe the pre fluid dynamical stages of heavy ion collisions at the highest SPS energies and above. The model predicts limited transparency for massive heavy ions.

Contrary to earlier expectations — based on standard string tensions of 1 GeV/fm which lead to the Bjorken model type of initial state — effective string tensions are introduced for collisions of massive heavy ions. The increased string tension is a consequence of collective effects related to QGP formation. These collective effects in central and semi central collisions lead to an effective string tension of the order of 10 GeV/fm and consequently cause much less transparency than earlier estimates. The resulting initial locally equilibrated state of matter in semi central collisions takes a rather unusual form, which can be then identified by the asymmetry of the caused collective flow. Our prediction is that this special initial state may be the cause of the recently identified "antiflow" or "third flow component".

Detailed fluid dynamical calculations as well as flow experiments at semi central impact parameters for massive heavy ions are needed at SPS and RHIC energies to connect the predicted special initial state with observables.

Acknowledgment

One of the authors (D.D.S.) thanks the support from the EU Research Infrastructure the Bergen Computation Physics Laboratory.

References

[1] L.P. Csernai, Zs. Lázár and D. Molnár, *Heavy Ion Phys.* **5** (1997) 467.

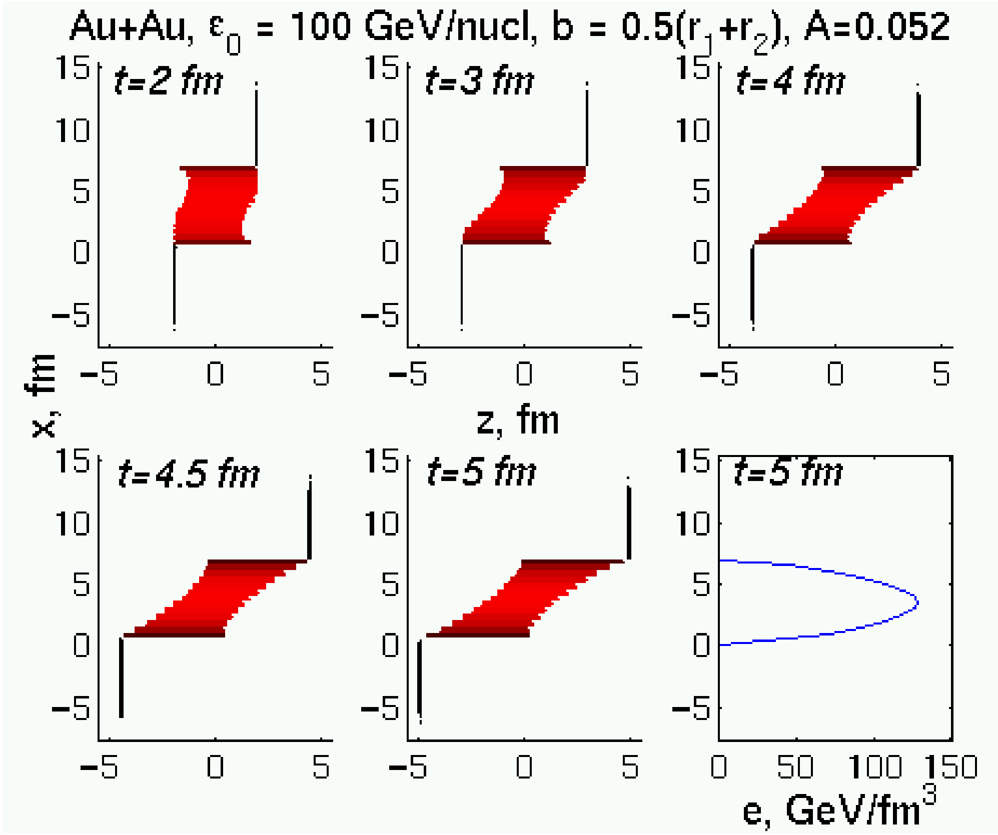

Figure 3: The Au+Au collision at $\varepsilon_0 = 100$ $GeV/nucl$, $b = 0.5(r_1 + r_2)$, $A = 0.052$ (parameter A was introduced in eq. (22)), $y = 0$ (ZX plane through the centers of nuclei). We note that the final shape of the QGP volume is a tilted disk $\approx 45^0$, and the direction of the fastest expansion will deviate from both the beam axis and the usual transverse flow direction and might be a reason for the third flow component, as argued in [17].

[2] Cs. Anderlik, Z.I. Lázár, V.K. Magas, L.P. Csernai, H. Stöcker and W. Greiner, *Phys. Rev.* **C59** (1999) 388. (nucl-th/9808024)

[3] V.K. Magas, Cs. Anderlik, L.P. Csernai, F. Grassi, W. Greiner, Y. Hama, T. Kodama, Zs. Lázár and H. Stöker, (nucl-th/9806004), *Phys. Rev.* **C59** (1999) 3309; (nucl-th/9903045), *Heavy Ion Phys.* **9** (1999) 193; (nucl-th/9905054), *Phys. Lett.* **B 459** (1999) 33.

[4] A.A. Amsden et al., *Phys. Rev.* **C17** (1978) 2080.

[5] L.P. Csernai et al., *Phys. Rev.* **C26** (1982) 149.

[6] J. Brachmann, S. Soff, A. Dumitru, H. Stöker, J.A. Maruhn, W. Greiner, D.H. Rischke, L. Bravina, *Phys. Rev.* **C61** (2000) 024909.

[7] T.S. Biró, H.B. Nielsen, J. Knoll, *Nucl. Phys.* **B245** (1984) 449.

[8] K. Werner, J. Aichelin, *Phys. Rev. Lett.* **76** (1996) 1027.

[9] N.S. Amelin, M.A. Braun, C. Pajares, *Phys. Lett.* **B306** (1993) 312, *Z. Phys.* **C63** (1994) 507.

[10] H. Sorge, *Phys. Rev.* **C52** (1995) 3291.

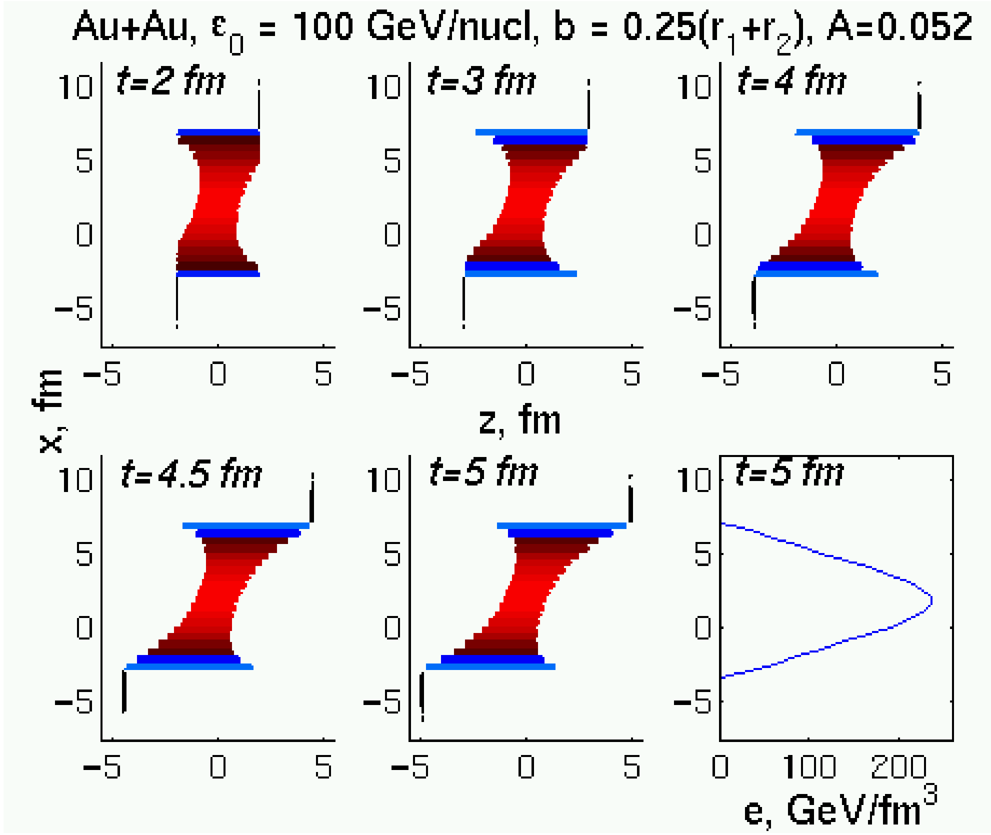

Figure 4: The same as Fig. 3, but $b = 0.25(r_1 + r_2)$. We see that for more central collisions the energy density is much larger. The QGP volume has a shape of tilted disk and may produce a third flow component [17].

[11] M. Gyulassy, L.P. Csernai, *Nucl. Phys.* **A460** (1986) 723.

[12] V.K. Magas, L.P. Csernai, D.D. Strottman, Proceedings of New Trends in High-Energy Physics, Yalta (Crimea), Ukraine, May 27 - June 4, 2000, p. 93. (nucl-th/0009049)

[13] L.P. Csernai, Cs. Anderlik, V.K. Magas, presented at the Symposium on Fundamental in Elementary Matter, Bad Honnef, Germany, September 25-29, 2000. (nucl-th/0010023)

[14] N. S. Amelin, E.F. Staubo, L.P. Csernai, V.D. Toneev, K.K. Gudima and D.D. Strottman, *Phys. Lett.* **B261** (1991) 352.

[15] N. S. Amelin, E.F. Staubo, L.P. Csernai, V.D. Toneev, K.K. Gudima and D.D. Strottman, *Phys. Rev. Lett.* **67** (1991) 1523.

[16] N.S. Amelin, L.P. Csernai, E.F. Staubo, and D. Strottman *Nucl. Phys.* **A544** (1992) 463c.

[17] L.P. Csernai, D. Röhrich, *Phys. Lett.* **B458** (1999) 454. (nucl-th/9908034)

[18] R.J.M. Snellings, H. Sorge, S.A. Voloshin, F.Q. Wang, N. Xu, *Phys. Rev. Lett.* **84** (2000) 2803-2805. (nucl-ex/9908001)

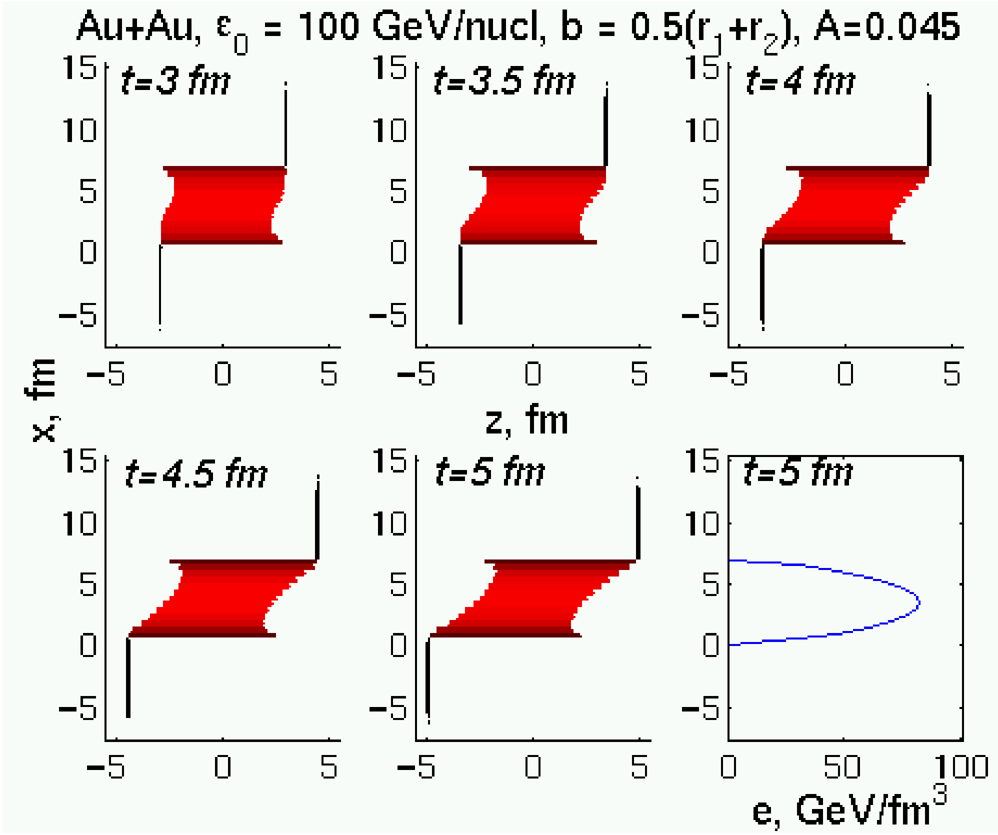

Figure 5: The same as Fig. 3, but $A = 0.045$. The energy density is smaller, but the QGP volume has a similar shape of a tilted disk $\approx 45^0$ and may produce a third flow component [17]. We start plotting our results later than in Fig. 4, because for smaller σ the deceleration is smaller, and, so, the final streak is formed later.

A Initial conditions after string creation

Our new conserved quantities are (27,28)

$$Q_0 = \int \tilde{T}^{00} dV = \triangle x \triangle y \sum_i \int_{l_i} \tilde{T_i}^{00} dz \ , \tag{42}$$

$$Q_3 = \int \tilde{T}^{03} dV = \triangle x \triangle y \sum_i \int_{l_i} \tilde{T_i}^{03} dz \ . \tag{43}$$

$$\tilde{T}^{00} = \frac{1}{4}\left(\tilde{T}^{++} + \tilde{T}^{+-} + \tilde{T}^{-+} + \tilde{T}^{--}\right) = \sum_i \tilde{T}_i^{00} \tag{44}$$

and

$$\tilde{T}^{03} = \frac{1}{4}\left(\tilde{T}^{++} - \tilde{T}^{+-} + \tilde{T}^{-+} - \tilde{T}^{--}\right) = \sum_i \tilde{T}_i^{03} \ . \tag{45}$$

Before string creation the initial values of the modified energy-momentum tensor, $\tilde{T}^{\mu\nu}$, are

$$\tilde{T}_1^{00} = \tilde{T}_2^{00} = e_0 \cosh^2 y_0 = \left(\frac{\varepsilon_0}{m}\right)^2 \rho_0 m \ , \tag{46}$$

$$\tilde{T}_2^{03} = -\tilde{T}_1^{03} = e_0 \cosh^2 y_0 = \left(\frac{\varepsilon_0}{m}\right)^2 \rho_0 m \tag{47}$$

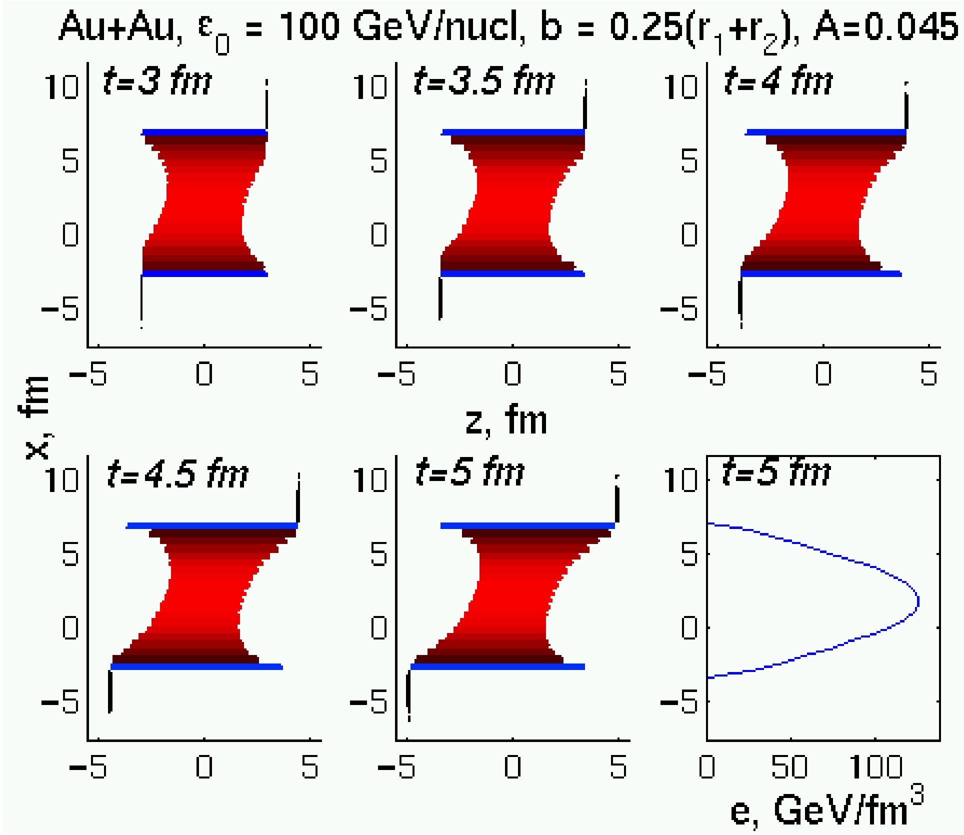

Figure 6: The same as Fig. 4, but $A = 0.045$. We see that for more central collisions – compared to Fig. 5 – the energy density is much larger, but it is smaller than in Fig. 4, because of smaller stopping. The QGP volume has a shape of tilted disk and may produce a third flow component [17].

where m is the nucleon mass, ε_0 is the initial energy per nucleon (ε means energy per nucleon, e means energy density). So,

$$Q_0 = \triangle x \triangle y \left(\frac{\varepsilon_0}{m}\right)^2 \rho_0 m (l_1 + l_2) \ , \tag{48}$$

$$Q_3 = \triangle x \triangle y \left(\frac{\varepsilon_0}{m}\right)^2 \rho_0 m (l_2 - l_1) \ , \tag{49}$$

where l_1 and l_2 are the initial lengths of streaks (see Fig 1), $\triangle x$, $\triangle y$ are the grid sizes in x and y directions.

After string creation

$$\tilde{T}_1^{00} = e_1 \cosh^2 y_1 + c_0^2 e_1 \sinh^2 y_1 + \frac{3}{2}\sigma^2 + \frac{\sigma x^-}{2} \rho_0 e^{y_0} \left(1 - 3e^{2y_1}\right) \ , \tag{50}$$

$$\tilde{T}_2^{00} = e_2 \cosh^2 y_2 + c_0^2 e_2 \sinh^2 y_2 + \frac{3}{2}\sigma^2 + \frac{\sigma x^+}{2} \rho_0 e^{y_0} \left(1 - 3e^{-2y_2}\right) \ , \tag{51}$$

$$\tilde{T}_{pert}^{00} = B \ , \tag{52}$$

$$\tilde{T}_1^{03} = e_1 (1 + c_0^2) \cosh y_1 \sinh y_1 + \sigma^2 - \frac{\sigma x^-}{2} \rho_0 e^{y_0} \left(1 - 3e^{2y_1}\right) \ , \tag{53}$$

$$\tilde{T}_2^{03} = e_2 (1 + c_0^2) \cosh y_2 \sinh y_2 - \sigma^2 + \frac{\sigma x^+}{2} \rho_0 e^{y_0} \left(1 - 3e^{-2y_2}\right) \ , \tag{54}$$

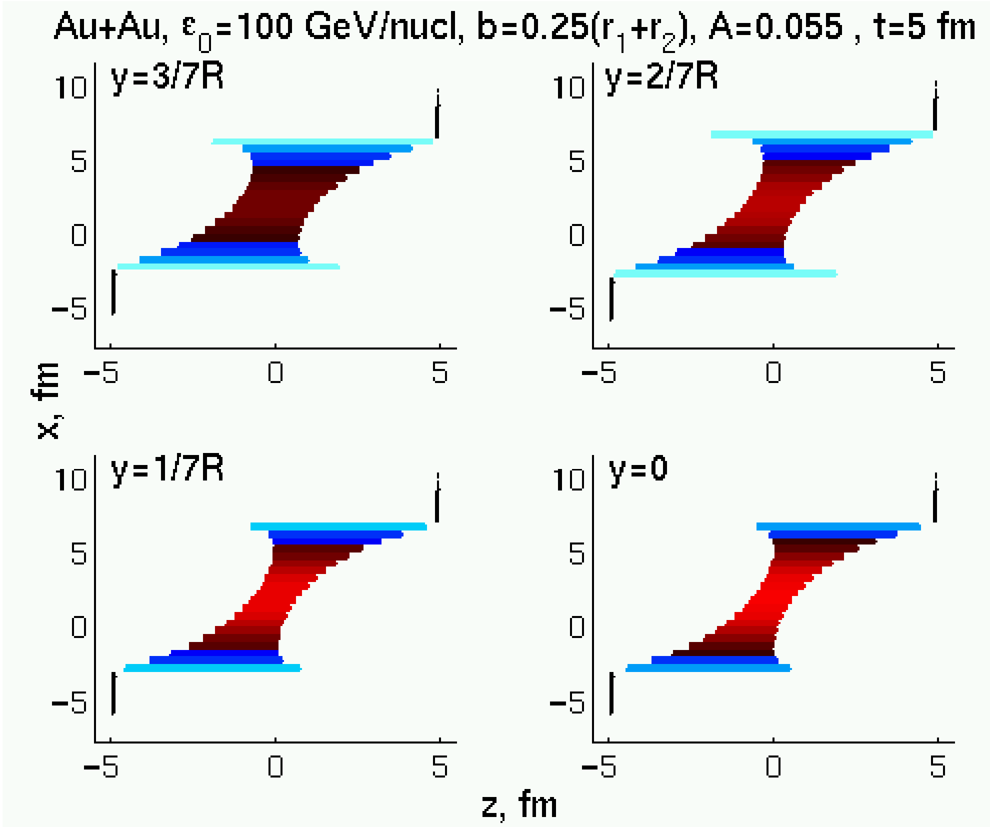

Figure 7: The Au+Au collision at $\varepsilon_0 = 100\ GeV/nucl$, $b = 0.25(r_1 + r_2)$, $t = 5\ fm$, $A = 0.055$ (parameter A was introduced in (22)). We see that the more central plane we look at, the more nucleons take part in the streak-streak collisions, and therefore the more energetic and compact QGP is formed.

$$\tilde{T}^{00}_{pert} = 0\ . \tag{55}$$

At the point of complete penetration of streaks, $t = t_0 = (l_1 + l_2)/2$ (see Fig 1), the conserved quantities Q_0 and Q_3 can be expressed through new parameters $\varepsilon_i(t_0)$, $\rho_i(t_0)$, $y_i(t_0)$, $\rho_i(t_0)$ (here we neglect $B \ll e_i$ and use $\cosh^2 y_i \approx \sinh^2 y_i = \left(\frac{\varepsilon_i(t_0)}{m}\right)^2 \gg 1$):

$$e_i(t_0) = m\rho_i(t_0)\ , \tag{56}$$

$$\rho_i(t_0)e^{-|y_i(t_0)|} = \rho_0 e^{y_0} \rightarrow \rho_i(t_0) = \rho_0 \frac{\varepsilon_0}{\varepsilon_i(t_0)}\ , \tag{57}$$

$$\frac{Q_0}{\triangle x \triangle y} = \left[\frac{3}{2}\sigma^2 + B\right](l_1 + l_2) + \frac{\sigma\rho_0 e^{y_0}}{8}\left((l_1 + l_2)^2 + 2l_1 l_2\right) + \rho_0\varepsilon_0(1 + c_0^2)\left(\left(\frac{\varepsilon_1(t_0)}{m}\right)l_1 + \left(\frac{\varepsilon_2(t_0)}{m}\right)l_2\right)\ , \tag{58}$$

$$\frac{Q_3}{\triangle x \triangle y} = -\sigma^2(l_2 - l_1) + \frac{\sigma\rho_0 e^{y_0}}{8}\left((l_2^2 - l_1^2\right) + \rho_0\varepsilon_0(1 + c_0^2)\left(\left(\frac{\varepsilon_2(t_0)}{m}\right)l_2 - \left(\frac{\varepsilon_1(t_0)}{m}\right)l_1\right)\ . \tag{59}$$

Then eqs. (58, 59) may be solved

$$\left(\frac{\varepsilon_1(t_0)}{m}\right) = \left(\frac{\varepsilon_0}{m}\right)\frac{1}{1 + c_0^2} - \frac{\sigma^2}{\rho_0\varepsilon_0(1 + c_0^2)}\frac{l_1 + 5l_2}{4l_1} - \frac{\sigma e^{y_0}}{8\varepsilon_0(1 + c_0^2)}(l_1 + 2l_2) - \frac{B}{\rho_0\varepsilon_0(1 + c_0^2)}\frac{l_1 + l_2}{2l_1}\ , \tag{60}$$

$$\left(\frac{\varepsilon_2(t_0)}{m}\right) = \left(\frac{\varepsilon_0}{m}\right)\frac{1}{1 + c_0^2} - \frac{\sigma^2}{\rho_0\varepsilon_0(1 + c_0^2)}\frac{l_2 + 5l_1}{4l_2} - \frac{\sigma e^{y_0}}{8\varepsilon_0(1 + c_0^2)}(l_2 + 2l_1) - \frac{B}{\rho_0\varepsilon_0(1 + c_0^2)}\frac{l_1 + l_2}{2l_2}\ . \tag{61}$$

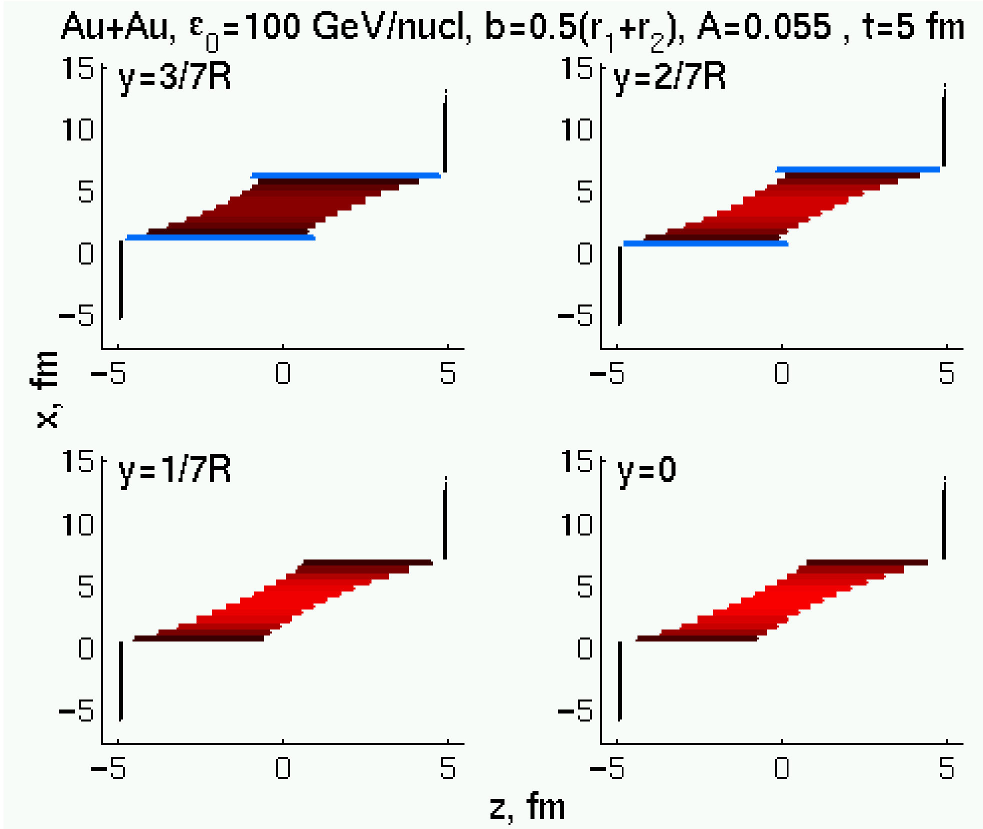

Figure 8: The same as Fig. 7, but $b = 0.5(r_1 + r_2)$. The stopping is smaller, consequently the QGP volume is less dense and less compact.

B The analytical solution of the model

For $x^{\pm} > x_0$ we should solve eqs. (24), based on boundary conditions (31). Eqs. (24) leads to the system of equations:

$$\partial_- \left(h_{1+} e^{-2y_1} \right) + \alpha \partial_+ h_{2+} = -2\sigma\rho_0 e^{y_0} + 2\sigma\rho_0 e^{y_0} e^{-2y_2} \ , \tag{62}$$

$$\alpha \partial_- h_{1+} + \partial_+ \left(h_{2+} e^{2y_2} \right) = 2\sigma\rho_0 e^{y_0} e^{2y_1} - 2\sigma\rho_0 e^{y_0} \ , \tag{63}$$

where $\alpha = (1 - c_0^2)/(1 + c_0^2)$. It is clear, that in both equations there are two terms depending on independent variables, so the solution will contain two undefined constants. The next step is to take eqs. (62, 63) at the values $x^+ = x_0$ and $x^- = x_0$.

$$h_{1+} = e^{2y_1} \left(e_1(t_0)(1 + c_0^2) e^{-2y_1(t_0)} - a_2(x^- - x_0) \right) \ , \tag{64}$$

$$\alpha \partial_+ h_{2+} = c_2 + 2\sigma\rho_0 e^{y_0} \left(e^{-2y_2} - e^{-2y_2(t_0)} \right) \ , \tag{65}$$

$$h_{2+} = e^{-2y_2} \left(e_2(t_0)(1 + c_0^2) e^{2y_2(t_0)} - a_1(x^+ - x_0) \right) \ , \tag{66}$$

$$\alpha \partial_- h_{1+} = c_1 + 2\sigma\rho_0 e^{y_0} \left(e^{2y_1} - e^{2y_1(t_0)} \right) \ , \tag{67}$$

where we introduced new notations

$$a_1 = c_1 + 2\sigma\rho_0 e^{y_0} - 2\sigma\rho_0 e^{y_0} e^{2y_1(t_0)} \ , \quad a_2 = c_2 + 2\sigma\rho_0 e^{y_0} - 2\sigma\rho_0 e^{y_0} e^{-2y_2(t_0)} \tag{68}$$

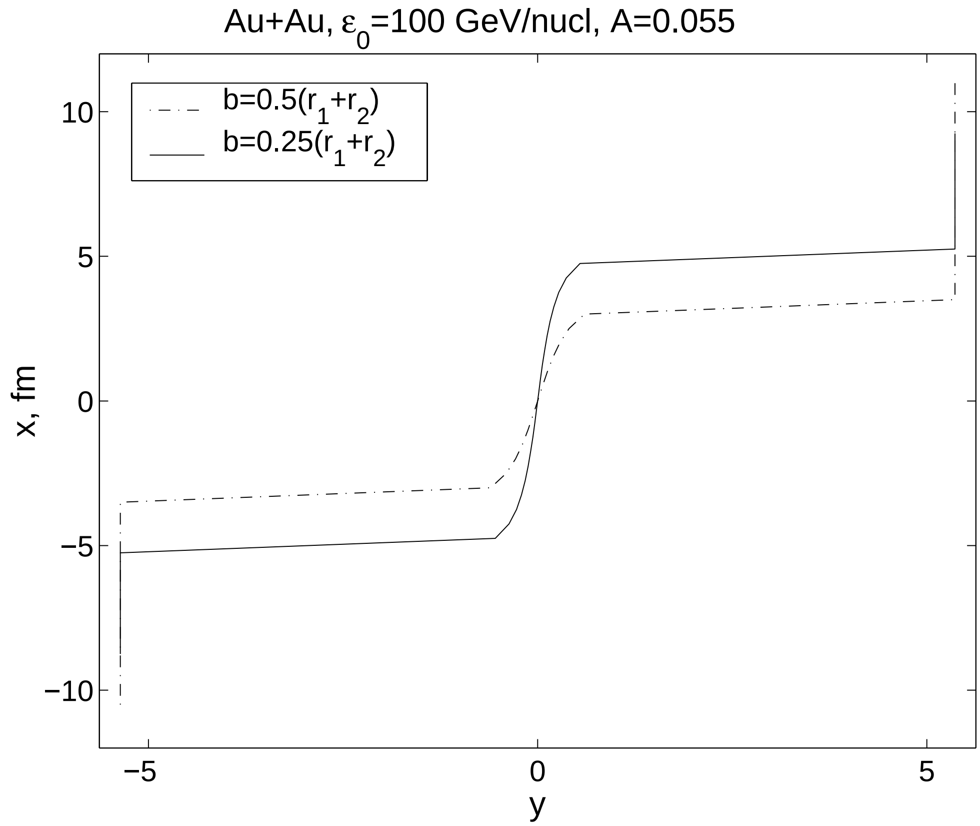

Figure 9: The rapidity profile of streaks in the reaction plane for Au+Au collision at $\varepsilon_0 = 100\ GeV/nucl$, $A = 0.055$, $y = 0$. The rapidities of the final streaks in CRF are calculated according to eq. (37). Our profiles are in agreement with schematical sketch in paper [18].

and two new constants

$$c_1 = \alpha(h_{1+})'|_{x_0}\ , \quad c_2 = \alpha(h_{2+})'|_{x_0}\ , \tag{69}$$

which will be estimated by assuming a linear development for the entalpy densities, h_{1+} and h_{2+}, from $t = 0$ ($x_\pm = |z(0)|$) to $t = t_0$ ($x_\pm = x_0$).

$$c_i = \alpha((1 + c_0^2)e_i(t_0) - e_0)/2t_0\ . \tag{70}$$

The complete analytical solution found to be

$$e^{(-)^{i+1}2y_i} = -\frac{d_i}{b_i} + \left(\frac{d_i}{b_i} + e^{(-)^{i+1}2y_i(t_0)}\right)\left(1 - \frac{x^i - x_0}{\tau_i}\right)^{-\frac{b_i}{\alpha a_j}}\ , \tag{71}$$

$$h_{i+} = e^{(-)^{i+1}2y_i} e_i(t_0)(1 + c_0^2)e^{-(-)^{i+1}2y_i(t_0)}\left(1 - \frac{x^i - x_0}{\tau_i}\right)\ , \tag{72}$$

$$\rho_i = \rho_0 e^{y_0} e^{(-)^{i+1}y_i}\ , \tag{73}$$

where $x^1 = x^-,\ x^2 = x^+,\ i,j = 1,2\ ,\ i \neq j$,

$$b_i = \alpha a_j + 2\sigma\rho_0 e^{y_0}\ , \tag{74}$$

$$d_i = c_i - 2\sigma\rho_0 e^{y_0} e^{(-)^{i+1}2y_i(t_0)}\ , \tag{75}$$

$$\tau_i = \frac{e_i(t_0)(1 + c_0^2)}{e^{(-)^{i+1}2y_i(t_0)}a_j}\ . \tag{76}$$